1994023385

N94-27888

MARS OZONE: MARINER 9 REVISITED

442634

Bernhard Lee Lindner

Atmospheric and Environmental Research, Inc.

840 Memorial Drive

Cambridge, Massachusetts 02139 USA

Telephone: (617)349-2280

Fax: (617)661-6479

Submitted to Geophys. Res. Lett.

Dec. 1993

No. of Pages: 12

No. of Figures: 3

No. of Tables: 0

ABSTRACT: The efficacy of the UV spectroscopy technique used by Mariner 9 to remotely measure ozone abundance at Mars is discussed. Previously-inferred ozone abundances could be underestimated by as much as a factor of 3, and much of the observed variability in the ozone abundance could be due to temporal and spatial variability in cloud and dust amount.

INTRODUCTION

Ozone is a key to understanding atmospheric chemistry on Mars. Over 20 photochemical models of the martian atmosphere have been published, and O_3 is often used as a benchmark for these models (e.g., Lindner, 1988; Shimazaki, 1989; Krasnopolsky, 1993). O_3 abundance has been inferred from instrumentation on several spacecraft, with the most complete coverage provided by Mariner 9 (Barth et al., 1973; Lane et al., 1973; Wehrbein et al., 1979). The Mariner 9 UV spectrometer scanned from 2100 to 3500 Angstroms with a spectral resolution of 15 Angstroms and an effective field-of-view of approximately 300 km^2. The only atmospheric absorption in the 2000 to 3000 Å wavelength region was previously assumed to come from the Hartley band system of ozone (Barth et al., 1973; Lane et al. 1973), which has an opacity of order unity at winter polar latitudes (Lindner, 1988). Therefore the amount of ozone was inferred by fitting this absorption feature with laboratory data of ozone absorption, as shown in Fig. 1 (Lane et al., 1973). Mars O_3 shows strong seasonal and latitudinal variation, with column abundances ranging from 0.2 μm-atm at equatorial latitudes to 60 μm-atm over northern winter polar latitudes (1 μm-atm is a column abundance of 2.689×10^{15} molecules cm^{-2}). However, the O_3 abundance is never great enough to significantly affect atmospheric temperatures (Lindner, 1991; 1993a) or surface temperatures and frost amounts (Lindner, 1990; 1992; 1993b). Figure 2 (Barth, 1985) shows some of the previously-inferred O_3 abundances.

MODELING PROCEDURE

A radiative transfer computer model is used to re-examine the Mariner 9 UV spectra. The discrete ordinate method of Stamnes et al. (1988) is used to treat the scattering and absorption of monochromatic radiation through the martian atmosphere. O_3 absorption cross-sections from 2000 Å to 3200 Å are included (Daumont et al., 1983; Freeman et al, 1984). Ultraviolet absorption cross-sections for CO_2, O_2, H_2O, HO_2 and H_2O_2 are negligible (e.g., Lindner, 1988; 1991;1993b). The Rayleigh scattering optical depth is computed as in Hansen and Travis (1974), using parameters appropriate for Mars. Atmospheric composition is taken as 95% CO_2 (Owen et al., 1977). The altitude dependence of O_3 is based on model results (Lindner, 1988).

Atmospheric properties are zonally averaged and assumed azimuthally-independent. The region from the surface to 40 km altitude is broken into twenty 2-km-thick layers to account for vertical inhomogeneity. The Chapman function is used to approximate the slant path in place of the secant function (Smith and Smith, 1972), because the winter polar atmosphere always has large solar zenith angles, and the secant function is in error for large angles. This work examines 57°N latitude in late winter (L_S = 343°), which is when the maximum O_3 column abundance was observed (Barth et al, 1973; Lane et al., 1973). [L_S, the solar longitude, is a seasonal index; L_s of 0°, 90°, 180°, 270°, correspond to northern spring equinox, summer solstice, autumnal equinox, and winter solstice, respectively]. The surface is covered by ice with an albedo of 0.6 (Warren and Wiscombe, 1980; Hapke et al., 1981; James and Lumme, 1982; Warren et al., 1990; Lindner, 1993a). The altitude profile of temperature rises linearly from 150K at the surface to 160K at 10 km, and then falls linearly with altitude to 130 K at 40 km, typical for winter polar conditions (Lindal et al., 1979; Kieffer, 1979).

Dust opacities varied from 0.2 to 1.0 for conditions other than global dust storms during the Mariner 9 and Viking observations (Briggs and Leovy, 1974; Pollack et al., 1979; Lumme and James, 1984), although dust opacities over winter polar latitudes may be slightly less [e.g., Lindner, 1990]. Dust opacity varies with wavelength (Zurek, 1978; 1982). The vertical distribution of dust is well-mixed to 20 km altitude (Anderson and Leovy, 1978; Zurek, 1982; Korablev et al., 1993). The single scattering albedo of airborne dust has a solar average of 0.9 (Clancy and Lee, 1991), but is only 0.6 in the 2000 Å to 3000 Å range (Pang et al., 1976; Thorpe, 1977). Scattering of radiation by dust is represented by the Henyey-Greenstein phase function, with an asymmetry parameter of 0.55 (Clancy and Lee, 1991). Typical cloud and fog opacities of 1.0 are taken from theory (Kulikov and Rykhletskii, 1983) and observations (Moroz, 1976; Pollack et al., 1977; Clancy and Lee, 1991), although large seasonal and latitudinal variations exist (Briggs and Leovy, 1974). A single-scattering albedo for cloud particles of 1.0 is taken from observations (Clancy and Lee, 1991). The Henyey-Greenstein phase function with asymmetry parameter of 0.55 is also used to describe the scattering by clouds (Clancy and Lee, 1991). Computational difficulties which accompany highly asymmetric phase functions are removed with the Delta-L method (Wiscombe, 1977).

RESULTS AND DISCUSSION

Using a constant mixing ratio for O_3 (e.g., Wehrbein, 1979; Lindner, 1988) and no chemical or radiative interaction between O_3 and clouds/dust, Fig. 3 shows that when typical amounts of dust and cloud are present that significant underestimation of O_3 abundance occurs. A factor of 3 times as much O_3 is needed to generate the same spectrum the spacecraft would measure for a cloudy, dusty atmosphere as for a clear atmosphere. If the scattering properties of martian clouds and dust were well known, then their appearance would not be a problem, as a model would be capable of retrieving the O_3 abundance. However, these properties are not well known, which raises doubts about the effectiveness of the UV reflectance spectroscopy technique for measuring O_3 abundance on Mars. The simulations shown in Fig. 3 are repeated for a range in solar zenith angle (50°-90°), ground albedo (0.3-0.8), altitude distribution of O_3, satellite viewing geometries, dust scattering properties, and cloud, dust and O_3 abundances. A factor of 3 underestimation is typical, with greater underestimation for high ground albedo or high dust opacities. Even if scattering by clouds is properly accounted for (as previously done with Mariner 9 data reduction in [4]), masking by dust can easily result in factor of 2 underestimation. Results are not strongly dependent on solar zenith angle.

Spatial and temporal variability in temperature and water vapor have been claimed to account for the scatter of the data points in Fig. 2 (Barth and Dick, 1974). A decrease in temperature results in a decrease in water vapor, assuming the atmosphere is saturated. A decreased water vapor abundance decreases the availability of odd hydrogen (H, OH, and HO_2), which converts CO and O into CO_2 catalytically, decreasing the abundance of O needed to form O_3. However, water vapor is a small source of odd hydrogen in the winter polar atmosphere compared to H_2, and may not account for most of the variability in Fig. 2 (Lindner, 1988). Masking by clouds and dust may also account for some of the observed O_3 variability, because the nature and opacity of the clouds and dust at winter polar latitudes change significantly spatially and temporally. As the maximum O_3 abundance resides near the surface (Lindner, 1988), spacecraft must be able to observe through the entire cloud and dust abundance in order to measure the total O_3 column abundance. If reflectance spectroscopy is used, as on Mariner 9, then the cloud and the airborne dust must be traversed twice; first by the incoming solar flux down to the surface, and then once again upon reflection from the surface out to the spacecraft. In addition, the large solar zenith angles at winter polar latitudes mean several times the vertical opacity of cloud and dust must be traversed. Indeed, part of the observed latitudinal variation in O_3 abundance in Fig. 2 may be due to the inability of the spacecraft to observe through the increasing effective optical depths as one goes poleward.

By using a photochemical model which included multiple scattering of solar radiation, Lindner (1988) showed that the absorption and scattering of solar radiation by clouds and dust should actually increase O_3 abundances at winter polar latitudes. Hence, regions with high dust and cloud abundance could contain high O_3 abundances (heterogeneous chemistry effects have yet to be fully understood [Atreya and Blamont, 1990; Krasnopolsky, 1993]). It is quite possible that the maximum O_3 column abundance observed by Mariner 9 of 60μm-atm is common. In fact, larger quantities may exist in some of the colder areas with optically thick clouds and dust. As the Viking period often had more atmospheric dust loading than did that of Mariner 9, the reflectance spectroscopy technique may even have been incapable of detecting the entire O_3 column abundance during much of the Mars year that Viking observed, particularly at high latitudes. The behavior of O_3 is virtually unknown during global dust storms, in polar night, and within the polar hood, leaving large gaps in our understanding.

Other possibilities for measuring O_3 abundance include solar occultation (Blamont et al., 1989), IR observations in the 9.6 μm O_3 absorption band (Espanek et al., 1991), and observations of the O_2 dayglow at 1.27 μm, produced by photolysis of O_3 (Traub et al., 1979). However, further studies of these other techniques are required, especially as regards the effects of clouds and dust.

ACKNOWLEDGMENTS. I thank Knut Stamnes for providing the radiative transfer program, and NASA's MSATT Program for support (contract NASW-4614).

REFERENCES

Anderson, E. and Leovy, C., Mariner 9 television limb observations of dust and ice hazes on Mars, *J. Atmos. Sci.*, **35**, 723-734, 1978.

Atreya, S.K. and Blamont, J.E., Stability of the martian atmosphere: Possible role of heterogenous chemistry, *Geophys. Res. Lett.*, **17**, 287-290, 1990.

Barth, C.A., Photochemistry of the atmosphere of Mars, in *The Photochemistry of Atmospheres. Earth, other Planets, and Comets,* ed. Levine, J., Academic Press, Orlando, Fla., 1985.

Barth, C.A. and Dick, M.L., Ozone and the polar hood of Mars, *Icarus*, **22**, 205-211, 1974.

Barth, C.A. C.W. Hord, A.I. Stewart, A.L. Lane, M.L. Dick and G.P. Anderson, Mariner 9 Ultraviolet experiment: Seasonal variation of ozone on Mars, *Science*, **179**, 795-796, 1973.

Blamont, J.E., E. Chassefiere, J.P. Goutail, B. Mege, M. Nunes-Pinharanda, G. Souchon, V.A. Krasnopolsky, A.A. Krysko and V.I. Moroz, Vertical profiles of dust and ozone in the martian atmosphere deduced from solar occultation measurements, *Nature*, **341**, 600-603, 1989.

Briggs, G.A. and Leovy, C.B., Mariner 9 observations of the Mars north polar hood, *Bull. Amer. Met. Soc.*, **55**, 278-296, 1974.

Clancy, R.T. and Lee, S.W., A new look at dust and clouds in the Mars atmosphere: Analysis of emission-phase-function sequences from global Viking IRTM observations, *Icarus*, **93**, 135-158, 1991.

Daumont, D., Brion, J. and Malicet, J., Measurement of total atmospheric ozone: Consequences entailed by new values of ozone absorption cross-sections at 223 K in the 310-350 nm spectral range, *Planet. Space Sci.*, **31**, 1229-1234, 1983.

Espanek, F., M.J. Mumma, T. Kostiuk, and D. Zipoy, Ground based infrared measurements of the global distribution of O3 in the atmosphere of Mars, *Icarus*, **92**, 252-262, 1991.

Freeman, D.E., K. Yoshino, J.R. Esmond and W.H. Parkinson, High resolution absorption cross-section measurements of ozone at 195 K in the wavelength region 240-350 nm, *Planet. Space Sci.*, **32**, 239-248, 1984.

Hansen, J.E. and Travis, L.D., Light scattering in planetary atmospheres, *Space Science Reviews*, **16**, 527-610, 1974.

Hapke, B., E. Wells, J. Wagner and W. Partlow, Far-UV, Visible, and Near-IR reflectance spectra of frosts of H_2O, CO_2, NH , and SO_2, *Icarus*, **47**, 361-367, 1981.

James, P.B. & Lumme, K., Martian south polar cap boundary: 1971 and 1973 data, *Icarus*, **50**, 368-380, 1982.

Kieffer, H.H., Mars south polar spring and summer temperatures: A residual CO_2 frost, *J. Geophys. Res.*, **84**, 8263-8288, 1979.

Korablev, O.I., V.A. Krasnopolsky, A.V. Rodin, and E. Chassefiere, Vertical structure of martian dust measured by solar infrared occulatations from the Phobos spacecraft, *Icarus*, **102**, 76-87, 1993.

Krasnopolsky, V.A., Photochemistry of the martian atmosphere (mean conditions), *Icarus*, **101**, 313-332, 1993.

Kulikov, Yu.N. and Rykhletskii, M.V., Modeling of the vertical distribution of water in the atmosphere of Mars, *Astron. Vestnik*, **17**, 144-152, 1983. (English translation: *Solar System Res.*, **17**, 112-118, 1983.)

Lane, A.L., Barth, C., Hord,C. and Stewart, A.I., Mariner 9 ultraviolet spectrometer experiment: Observations of ozone on Mars, *Icarus*, **18**, 102-108, 1973.

Lindal, G.F., H.B. Hotz, D.N. Sweetnam, Z. Shippony, J.P. Brenkle, G.V. Hartsell, R.T. Spear and W.H. Michael, Jr., Viking radio occultation measurements of the atmosphere and topography of Mars: Data acquired during 1 martian year of tracking, *J. Geophys. Res.*, **84**, 8443-8456, 1979.

Lindner, B.L., Ozone on Mars: The effects of clouds and airborne dust, *Planet. Space Sci.*, **36**, 125-144, 1988.

Lindner, B.L., The martian polar cap: Radiative effects of ozone, clouds, and airborne dust, *J. Geophys. Res.*, **95**, 1367-1379, 1990.

Lindner, B.L., Ozone heating in the martian atmosphere, *Icarus*, **93**, 354-361, 1991.

Lindner, B.L., Sunlight penetration through the martian polar caps: Effects on the thermal and frost budgets, *Geophys. Res. Lett.*, **19**, 1675-1678, 1992.

Lindner, B.L., The hemispherical asymmetry in the martian polar caps, *J. Geophys. Res.*, **98**, 3339-3344, 1993a.

Lindner, B.L., Martian atmospheric radiation budget, submitted to *Publ. Astron. Soc. Japan*, 1993b.

Lumme K. and James, P.B., Some photometric properties of the martian south polar cap region during the 1971 apparition, *Icarus*, **58**, 363-376, 1984.

Moroz, V.I., Clouds on Mars: Some results from observations on Mars 3, *Kosmich. Issled.*, **14**, 406-416, 1976. (English translation: *Cosmic Res.*, **14**, 364-372, 1976).

Owen, T., K. Biemann, D.R. Rushneck, J.E. Biller, D.W. Howarth, and A.L. Lafleur, The composition of the atmosphere at the surface of Mars, *J. Geophys. Res.*, **82**, 4635-4639, 1977.

Pang, K., J. M. Ajello, C.W. Hord, and W.G. Egan, Complex refractive index of martian dust: Mariner 9 UV observations, *Icarus*, **27**, 55-67, 1976.

Pollack, J.B., D. Colborn, R. Kahn, J. Hunter, W. Van Camp, C.E. Carlston and M.R. Wolf, Properties of aerosols in the Martian atmosphere as inferred from Viking Lander imaging data, *J. Geophys. Res.*, **82**, 4479-4496, 1977.

Pollack, J.B., D.S. Colburn, F.M. Flasar, R. Kahn, C.E. Carlston and D. Pidek, Properties and effects of dust particles suspended in the martian atmosphere, *J. Geophys. Res.*, **84**, 2929-2945, 1979.

Shimazaki, T., Photochemical stability of CO2 in the martian atmosphere: Reevaluation of the eddy diffusion coefficient and role of water vapor, *J. Geomag. Geoelectr.*, **41**, 273-301, 1989.

Smith, F.L., III, and Smith, C., Numerical evaluation of Chapman's grazing incidence integral ch(X,X), *J. Geophys. Res.*, **77**, 3592-3597, 1972.

Stamnes, K., S. Tsay, W. Wiscombe, and K. Jayaweera, Numerically stable algorithm for discrete-ordinate-method radiative transfer in multiple scattering and emitting media, *App. Optics*, **27**, 2502-2509, 1988.

Thorpe, T.E., Viking orbiter observations of atmospheric opacity during July-November 1976, *J. Geophys. Res.*, **82**, 4151-4159, 1977.

Traub, W.A., N.P. Carleton, P. Connes and J.F. Noxon, 1979: The latitudinal variation of O2 dayglow and O3 abundance on Mars, *Astrophys. J.*, **229**, 846-850, 1979.

Warren, S.G. and Wiscombe, W.J., A model for the spectral albedo of snow. II: Snow containing atmospheric aerosols, *J. Atmos. Sci.*, **37**, 2734-2745, 1980.

Warren, S.G., W.J. Wiscombe, and J.F. Firestone, Spectral albedo and emissivity of CO2 in martian polar caps: model results, *J. Geophys. Res.*, **95**, 14717-14741, 1990.

Wehrbein, W.M., C.W. Hord, and C.A. Barth, Mariner 9 UV Spectrometer Experiment: Vertical distribution of ozone on Mars, *Icarus*, **38**, 288-299, 1979.

Wiscombe, W.J., The delta-m method: Rapid yet accurate radiative flux calculations for strongly asymmetric phase functions, *J. Atmos. Sci.*, **34**, 1408-1422, 1977.

Zurek, R.W., Solar heating of the martian dusty atmosphere, *Icarus*, **35**, 196-208, 1978.

Zurek, R.W., Martian great dust storms: An update, *Icarus*, **50**, 288-310, 1982.

FIGURE CAPTIONS

Figure 1. Ultraviolet spectrum measured by Mariner 9 at 57°N latitude on orbit 144 (taken from Lane et al., 1973). To enhance the O_3 absorption feature, this spectrum was divided by one obtained at 20°N latitude on orbit 144, where O_3 abundances are minimal.

Figure 2. Measurements of the O_3 column abundance previously inferred from the Mariner 9 UV spectrometer data during the northern winter, L_s = 330-360°, in the northern hemisphere (taken from Barth, 1985).

Figure 3. Synthetic spectra as would be observed by spacecraft for atmospheres with no cloud or dust and 30 μm-atm O_3 (solid line), vertical opacities of dust and cloud of 0.3 and 1.0, respectively, and 30 μm-atm of O_3 (dashed line), and vertical opacities of dust and cloud of 0.3 and 1.0, respectively, and 100 μm-atm of O_3 (dotted line). All cases assume a solar a zenith angle of 75° (typical for winter polar observations), and a polar cap albedo of 0.6.

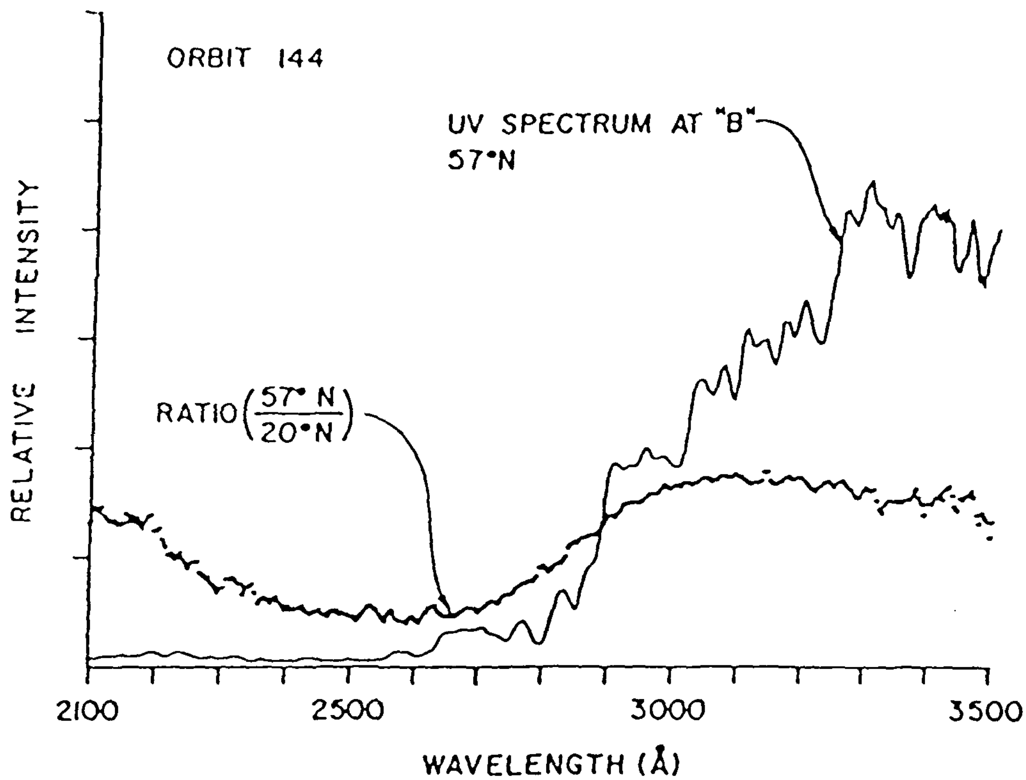
ORBIT 144
UV SPECTRUM AT "B"
57°N
RATIO (57° N / 20° N)
RELATIVE INTENSITY
2100
2500
3000
3500
WAVELENGTH (Å)

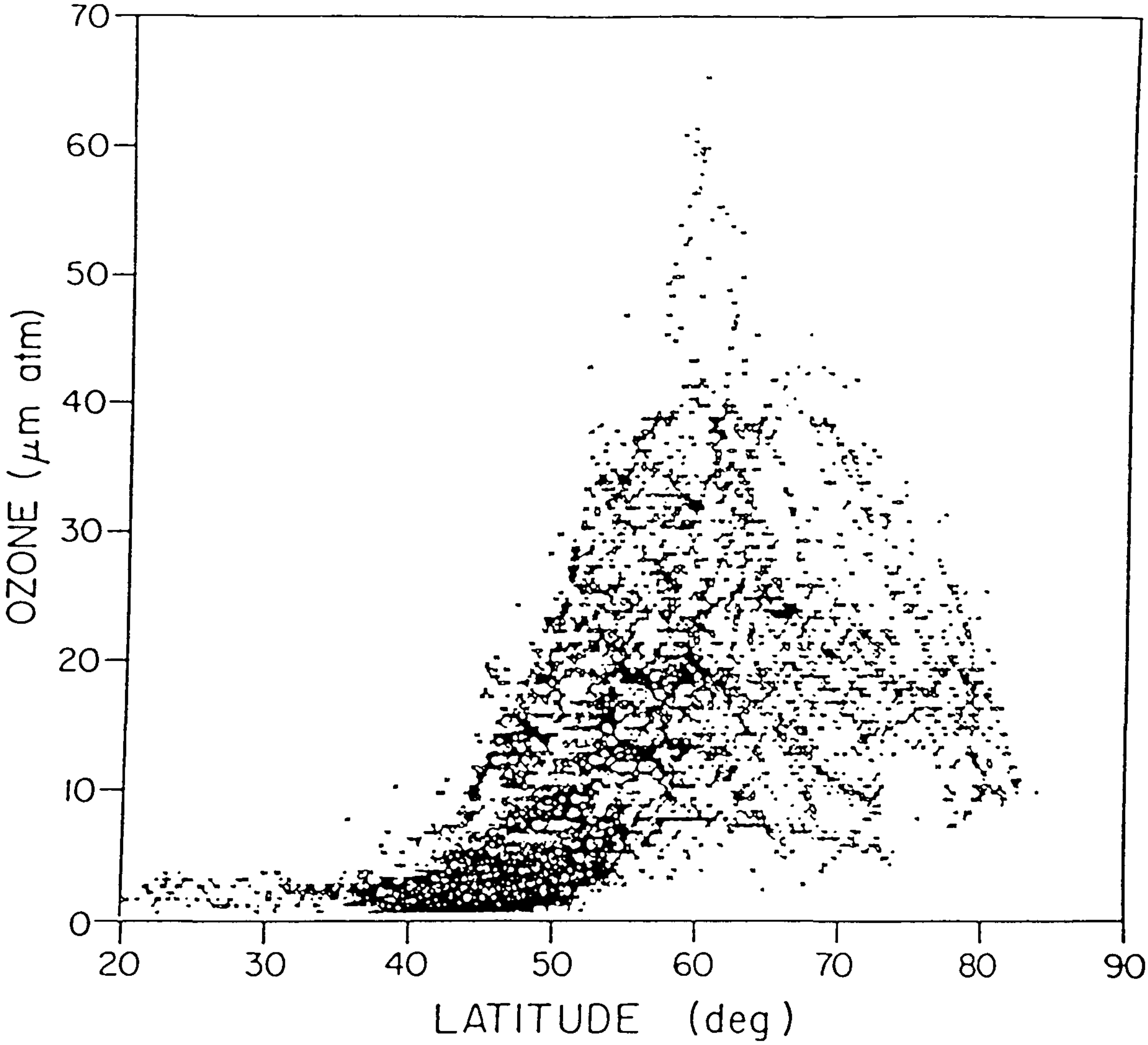

70
60
50
40
30
20
10
0
OZONE (μm atm)
20
30
40
50
60
70
80
90
LATITUDE (deg)

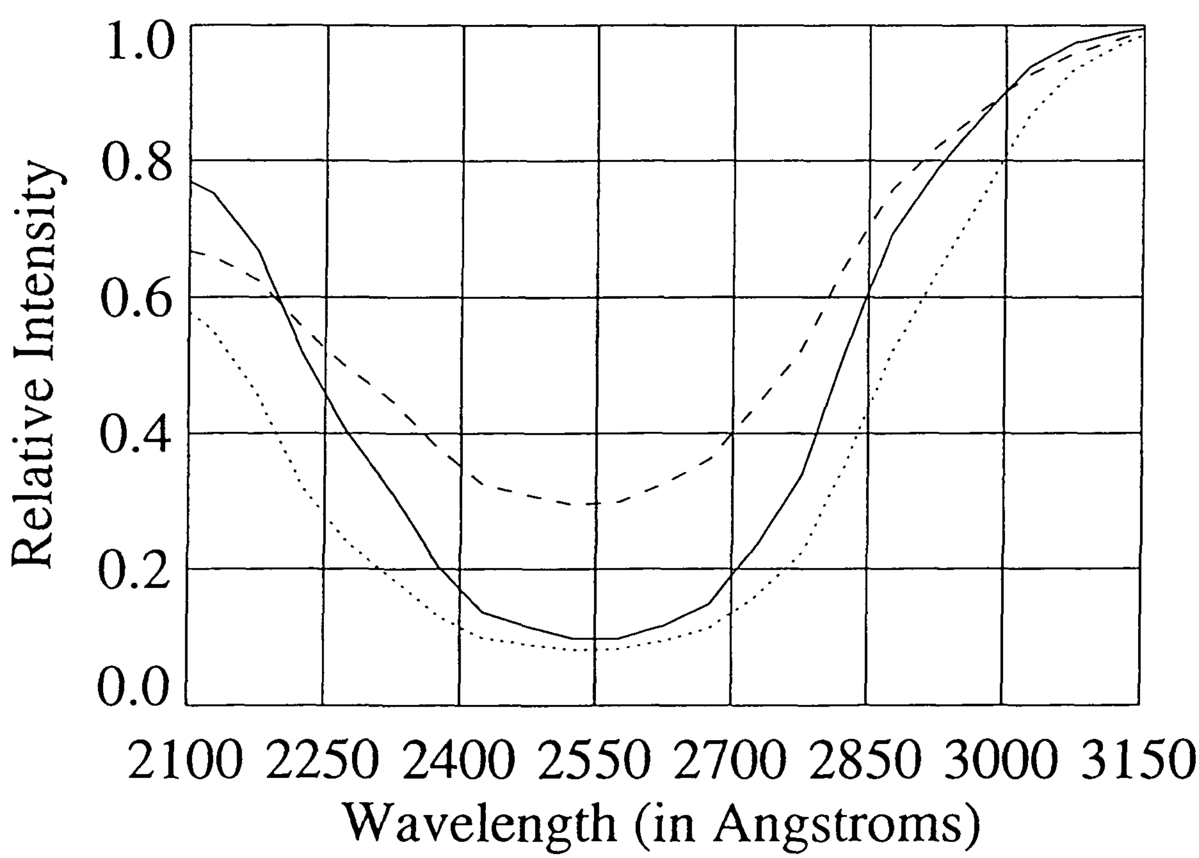
1.0
0.8
0.6
0.4
0.2
0.0
Relative Intensity
2100 2250 2400 2550 2700 2850 3000 3150
Wavelength (in Angstroms)